



Making of zeolite membranes for the dehydration of azeotropic solvents

Mansoor Kazemimoghadam

Malek Ashtar University of Technology, Tehran, Iran

Abstract

Zeolite membranes NaA, ZSM-5, Mordenite, NaX and NaY grown onto seeded mullite supports. Separation performance of zeolite membranes were studied for water-dimethylhydrazine mixtures using pervaporation (PV). The best Flux and separation factor of the membranes were 0.62 kg/m².h and 52000, respectively, for NaA zeolite membrane. Strong electrostatic interaction between ionic sites and water molecules (due to its polar nature) makes the zeolite NaA membrane very hydrophilic. Zeolite NaA membranes are thus well suited for separating liquid-phase mixtures by pervaporation. In this study, experiments were conducted with various dimethylhydrazine –water mixtures (1–20 wt. %) at 25^oC. Total flux for UDMH–water mixtures was found to vary from 0.331 to 0.241 kg/m².h with increasing UDMH concentration from 1 to 20 wt.%. Ionic sites of the NaA zeolite matrix play a very important role in water transport through the membrane. Surface diffusion of water occurs in an activated fashion through these sites. A comparison between experimental flux and calculated flux using Stephan Maxwell (S.M.) correlation was made and a linear trend was found to exist for water flux through the membrane with UDMH concentration. © 2017 ijrei.com. All rights reserved

Keywords: Nanopore; Pervaporation; Zeolite membranes; Stephan Maxwell model

1. Introduction

Pervaporation is an economical separation technique compared to conventional separation methods such as distillation especially in processes involving azeotropes, isomers and removal or recovery of trace substances. Due to its high separation efficiency and flux rates, PV results in energy cost saving and safe operation. In this regard, pervaporation eliminates the use of toxic materials and is a promising alternative for energy consuming distillation processes in separating azeotropic mixtures. Table 1 shows energy consumptions required by different separation methods in ethanol dehydration. In terms of energy requirement, pervaporation is an obvious choice in ethanol–water separation. Furthermore, PV has several advantages over traditional distillation: (1) reduced energy demand because only a fraction of the liquid that needs to be separated is vaporized, (2) simple equipment since only a vacuum pump is used to create a driving force and (3) lower capital cost. Thus, relatively mild operation conditions and high effectiveness make PV an appropriate technique for such separations. As a result, most PV studies have been focused on dehydration of organic mixtures. In PV, the feed mixture is contacted with a nonporous permselective membrane. Separation is, in general,

explained by the steps of sorption into, diffusion through and desorption from the membrane. The latter is usually considered to be fast and taking place at equilibrium, while diffusion is kinetically controlled and the slowest step of the process. Permeation is dependent on sorption and diffusion steps. The driving force for the separation is created by maintaining a pressure lower than the saturation pressure on the permeate side of the membrane. The mechanism of separation is usually explained in terms of sorption-diffusion processes [1-3].

UDMH is an important solvent; however it also finds many new applications as an oxygen scavenger for boiler-feed water, a starting material for drug and dye intermediates, a catalyst for polymerization reactions, etc. UDMH is very corrosive and its vapor is extremely toxic and carcinogenic.

Membrane-based PV technology has all the requirements for completely replacing extractive distillation for separation of the azeotropes. This can be combined with simple distillation as a hybrid process for enrichment of UDMH to high purity levels. Chitosan, a derivative of the naturally abundant biopolymer chitin, is fully stable in anhydrous UDMH and hence can be selected for its dehydration, keeping in minds its highly hydrophilic nature and good mechanical strength. The

promising potential of chitosan as a PV membrane has already been exploited for dehydration of alcohols such as ethanol and isopropanol. This polymer has recently been used to form selective and permeable blend membranes with poly (vinyl alcohol), sodium alginate, etc. However, unfortunately polymeric membranes behaved unsuitable in terms of selectivity and flux in general for water-UDMH mixtures (selectivity and flux of about 10 and 0.01 kg/m².h, respectively) [4,5].

Polyphenylene oxide (PPO) membranes synthesized from 2, 6-dimethyl phenol monomer were subjected to pervaporation-based dehydration of the UDMH mixtures. Separation factors (35–70) and water fluxes (0.1–0.2 kg/m² h) were observed for separation of the aqueous azeotropes of UDMH (20 wt. %) [6]. Polymeric membranes are not generally suitable for applications involving harsh solvents like UDMH due to membrane chemical instability. However, a recent development of solvent-and-temperature resistant hydrophilic ceramic membranes made it possible to overcome the limitations of hydrophilic polymeric membranes. PV is an economical separation technique compared with conventional separation methods such as distillation especially in processes involving azeotropes, isomers and (removal or recovery of) trace substances. Due to its high separation factor and flux, PV results in energy cost saving and safe operation. In PV, feed mixture is contacted with a nonporous permselective membrane. Separation is, in general, explained by the steps of sorption into, diffusion through and desorption from the membrane. The latter is usually considered to be fast and taking place at equilibrium, while diffusion is kinetically controlled and the slowest step of process. Permeation depends on sorption and diffusion steps. Driving force for the separation is created by maintaining a pressure lower than saturation pressure on permeate side of the membrane. The mechanism of separation is usually explained in terms of sorption-diffusion processes [7].

However, a recent development of chemical-and-temperature resistant hydrophilic ceramic membranes has made it possible to overcome the limitations of hydrophilic polymeric membranes. Zeolite membranes are another kind of pervaporation materials for separating water from highly concentrated ethanol aqueous solution since zeolites are most hydrophilic and have well-defined open crystal structures with a pore size of several angstroms. These unique structural characteristics and hydrophilic nature have rendered zeolite materials possessing pronounced molecular sieving effect and selective adsorption capability (i.e., appreciated separation performance). Therefore, zeolites can be extensively applied in removal of volatile organic chemicals from air streams, separation of isomers and mixtures of gases, shape-selective catalysis and ion exchange. The zeolitic membranes offer several advantages over polymeric ones: (i) they do not swell significantly compared to polymeric membranes, (ii) they have uniform molecular-sized pores that provide differential transport rates and molecular sieve effects, (iii) the zeolitic structures are more chemically stable, tolerant to harsh separation conditions such as strong solvents or low pH, (iv)

zeolites are thermally stable up to high temperatures of 1000°C. Nano and uniform pore size of these zeolites makes separation of small molecules possible via molecular sieving. Zeolite membranes were found to be extremely effective for dehydration of ethanol by PV, with separation factors of 10⁴ or more being achieved. This has many potential advantages in terms of reproducibility and easy control [8].

This paper focuses on separation of UDMH–water mixtures using zeolite membranes and comparison of these membranes. In addition, a comparison FOR NaA zeolite membrane between experimental flux and calculated flux using S.M. Correlation was made and a linear trend was found to exist for water flux through the membrane with UDMH concentration.

2. Experimental

2.1 Support preparation

In ceramic membranes, thin dense layers are usually deposited over porous supports. The porous supports provide mechanical strength for the thin selective layers. Porous supports can be made from alumina, cordierite, mullite, silica, spinel, zirconia, other refractory oxides and various oxide mixtures, carbon, sintered metals and silicon carbide.

In this research, mullite supports have been prepared from kaolin clay. Kaolin is thermally converted to mullite via high temperature calcinations. The reaction takes place when kaolin is utilized as the sole source of silica and alumina. The reaction can be represented by the following equation:



Free silica (4SiO₂) is generated as a result of this conversion. The free silica has been leached out and then porous mullite bodies have been prepared. Mullite has several distinct advantages over other materials. Since kaolin is heated to high temperatures to achieve the mullite conversion reaction, strong inter-crystalline bonds between mullite crystals are formed and this results in excellent strength and attrition. Leaching time depends on several factors including:

- (1) The quantity of free silica to be removed,
- (2) the porosity of body prior to leaching,
- (3) the concentration of leaching solution and
- (4) Temperature.

Kaolin (SL-KAD grade) has been supplied by WBB cooperation, England. Analysis of the kaolin is listed in Table 2. Cylindrical shaped (tubular) bodies (ID: 10 mm, OD: 14 mm and L: 15 cm) have been conveniently made by extruding a mixture of about 75-67% kaolin and 25-33% distilled water. Suitable calcinations temperatures and periods are those at which kaolin converts to mullite and free silica. Good results have been achieved by calcining for about 3 h at temperatures of about 1250°C (Figure 1).

Free silica has been removed from the calcined bodies after leaching by strong alkali solutions. Removal of the silica

causes mesoporous tubular supports to be made with very high porosity. Free silica removal has been carried out using aqueous solutions containing 20% by weight NaOH at a temperature of 80 °C for 5 h [9, 10]. Supports have been rinsed using a lot of hot distilled water for a long time in order to remove the all-remaining NaOH. Porosity of the supports before leaching is 24.3%, while after treatment it increases to 49%. Flux of the supports before and after free silica removal at 1 bar and 20 °C is 6 kg/m²h and 10 kg/m²h, respectively.

Porosity of the supports has been measured by water absorption method. The phases Mullite, Cristobalite and SiO₂ identification was performed by XRD (Philips PW1710, Philips Co., Netherlands) with CuK α radiation. Morphology of the support and the membrane was examined by SEM (JEM-1200 or JEM-5600LV equipped with an Oxford ISIS-300 X-ray disperse spectroscopy (EDS)). Phase identification has been performed by X-ray diffractometry with CuK α radiation. Figure 2 shows XRD of the mullite support synthesized using the above-mentioned method. It has been shown morphology of support by SEM micrograph as shown in Figure 3.

2.2 Synthesis of zeolite membranes

Thin zeolite membranes layers were grown hydro thermally over the external surface of the porous supports. Synthesis solution was prepared by mixing aluminates and silicate solutions. For membrane preparation, after preparation a homogeneous gel, two ends of the support was closed with rubber caps to avoid any precipitation of the zeolite crystals on inner surface of the supports during membrane synthesis. The support was placed vertically in a Teflon autoclave. The solution was carefully poured in to the autoclave and then the autoclave was sealed. Crystallization was carried out in an oven at a constant temperature. Then, the samples were taken and the synthesized membranes were washed several times with distilled water. The sample was then dried at room temperature for 12 h in air and then dried in the oven at 100 °C for 15 h to remove water occluded in the zeolite crystals. Gel Formulations of zeolite membranes show in table 3.

2.2.1 ZSM-5

The ZSM-5 molar gel composition was 0.292Na₂O:1.0Al₂O₃:100SiO₂:2.0-5.0TPABr: 40-65H₂O, where tetra propyl ammonium bromide (TPABr) was used as template. Sodium silicate and sodium aluminates were used as the Si and Al sources, respectively. For ZSM-5 preparation, three solutions were used, solution A: sodium silicate; solution B: TPABr + H₂O (half of the total water); solution C: NaOH + Na₂Al₂O₄ + H₂O (other half of the water). Solution A was added to solution B and then solution C was added while stirring. To obtain a homogeneous gel, the mixture was stirred for 2 h at room temperature. After synthesis of membrane, sample was calcined in air at 530 oC for 8 h at a heating rate of 1 °C /min [11-14].

Figure 4 show XRD pattern of the ZSM-5 zeolite membrane.

Morphology of the membrane subjected to crystallization was characterized by SEM. Figure 5 shows morphology of the ZSM-5 membrane (surface of membrane). As seen, most of the crystals lie disorderly on the surface.

2.2.2 Mordenite

The mordenite zeolite membranes were synthesized on the outer surface of the porous mullite tubes. Synthesis solution was prepared by mixing aluminates and silicate solutions. NaOH was dissolved in distilled water. The solution was divided into two equal volumes and kept in polypropylene bottles. Aluminate solution was prepared by adding sodium aluminates to one part of the NaOH solution. It was mixed until cleared. Silicate solution was prepared by adding sodium silicate to another part of the NaOH solution. Silicate solution was then poured into aluminate solution and well mixed until a thick homogenized gel was formed. Molar composition of the starting gel of the mordenite zeolite membranes was SiO₂/Al₂O₃=9-30, Na₂O/SiO₂=9.75, H₂O/Na₂O=780. Crystallization was carried out in an oven at a temperature of 170 °C for 24 h. Then, the samples were taken and the synthesized membranes were washed several times with distilled water. The samples were then dried at room temperature in air and then dried in the oven at 100 °C for 15 h prior to characterization and evaluation [15-16].

Figure 6 shows XRD pattern of the mordenite zeolite membrane. Morphology of the membrane subjected to crystallization was characterized by SEM (Figure 7). The SEM photograph of the mordenite membrane (surface) shows that the mullite surface is completely covered by a mordenite crystal layer.

2.2.3 Faujasite

Molar composition of the starting gel of the NaX and NaY zeolite membranes were SiO₂/Al₂O₃=2.5, Na₂O/SiO₂=2, H₂O/Na₂O=200 and SiO₂/Al₂O₃=10, Na₂O/Al₂O₃=4, H₂O/Al₂O₃=250 respectively [17,18].

Crystallization was carried out in an oven at a temperature of 100°C at period duration for 6 h and 24 for NaX and NaY respectively. Figures 8 and 9 show XRD patterns of the NaX and NaY zeolite membrane. Figures 10 and 11 show morphology of the Faujasite (NaX and NaY) membranes (surface section). As seen, most of the crystals lie disorderly on the surface. The SEM photograph of the Faujasite (NaX and NaY) membranes (cross section) show that the mullite surface is completely covered by a zeolite crystal layer.

2.2.4 NaA

NaOH (4.87 g) was dissolved in 76 ml of distilled water. The solution was divided into two equal volumes and kept in polypropylene bottles. Aluminates solution was prepared by adding 6.23 g sodium aluminates (Aldrich, 50-56% Al₂O₃) to one part of the NaOH solution. It was mixed until cleared.

Silicate solution was prepared by adding 16.57 g sodium silicate (Merck, 25-28% SiO₂) to another part of the NaOH solution. Silicate solution was then poured into aluminates solution and well mixed until a thick homogenized gel was formed. Composition of the homogeneous solution of zeolite NaA is represented by the following molar ratio: 1.926 SiO₂: Al₂O₃: 3.165 Na₂O: 128 H₂O [19-21].

Crystallization was carried out in an oven at temperature of 100, for 3 h. Then, the sample was taken and the synthesized membrane was washed several times with distilled water. The sample was then dried at room temperature for 12 h in air.

The XRD pattern of NaA zeolite membranes confirm that crystal of zeolite NaA has been formed. Figure 12 shows XRD of the mullite support and membranes synthesized using the above-mentioned methods. In this figure, the only phases, which can be observed, are zeolite NaA and mullite. It has been shown morphology of support and membrane by SEM micrograph. Figure 13 shows SEM photographs of the mullite support and NaA zeolite membrane (surface and cross section). Porous structure of the support and thin layer of the membrane can be easily observed.

2.3 Pervaporation experiments

A PV experimental set up was used to evaluate successful fabrication of zeolite membranes. PV experiments were carried out using a standard PV apparatus. Feed solution, preheated to a constant temperature, was introduced to the outer side of the zeolite membrane in the PV cell. The downstream pressure was maintained at 133 Pa throughout the operation. The zeolite membranes were used for dehydration of aqueous UDMH mixtures. The UDMH mixtures (2 and 5 wt%) were used and experiments were carried out at room temperature (25°C) within a period of 30-60 min. Permeate concentrations were measured using GC (TCD detector, Varian 3400, carrier gas: hydrogen, column: polyethylene glycol, sample size: 5 micron, column and detector temperatures: 120-150°C, detector flow rate: 15 ml/min, carrier flow: 5 ml/min, column pressure: 1.6 kPa, GC input pressure: 20 kPa). Performance of PV was evaluated using values of total flux (kg/m².h) and separation factor (dimensionless). Typical experimental setup was employed as presented in Figure 14.

Performance of PV is usually evaluated by total flux (kg/m².h) and separation factor (dimensionless). Separation factor of any organic aqueous solution can be calculated from the following equation:

$$\text{Separation factor } (\alpha) = \frac{\left[\frac{X_{H_2O}}{X_{Organic}} \right]_{\text{permeate}}}{\left[\frac{X_{H_2O}}{X_{Organic}} \right]_{\text{feed}}}$$

Where X_{H_2O} and $X_{organic}$ are weight fractions of water and organic compound, respectively. The Comparison of Zeolite membranes for dehydration of UDMH/water mixtures by pervaporation setup presented in table 4. AS shown in table

4, NaA Zeolite membrane is the best Zeolite for separation these mixtures.

3. Experimental results and Stephan Maxwell Model for NaA zeolite membrane

3.1 NaA Zeolite structure and transport mechanisms

The hydrophilic membranes used in this research were composite zeolite NaA membranes. The membranes were basically made of an active NaA layer, deposited on a ceramic porous mullite support. The active NaA layer is responsible for high separation factors achieved in PV of UDMH mixtures. The structure of zeolite NaA is shown in Figure 15.

As shown in Figure 15, the aluminosilicate framework of zeolite NaA is generated by placing truncated octahedrons (b-cage) at eight corners of a cube and each edge of the cube is formed by joining two b-cages by a D4R linkage. Each b-cage encloses a cavity with a free diameter of 0.66 nm and each unit cell encloses a larger cavity (a-cage) enclosing a free diameter of 1.14 nm. There are two interconnecting, three-dimensional channels in zeolite NaA: (i) connected a-cages, 1.14 nm in diameter, separated by 0.42 nm apertures, (ii) b-cages, alternating with a-cages separated by 0.22 nm apertures. Thus, molecules smaller than 0.42 nm in diameter can diffuse easily through the nanopores of the zeolite. In addition, position of sodium ions in unit cells is important since these ions act as the sites for water sorption and transport through the membrane. For a typical zeolite, a unit cell having the composition Na₁₂Al₁₂Si₁₂O₄₈.27H₂O, eight (out of 12) sodium ions are located inside an a-cage and four ions are located in b-cages. Transport of solvent species (mainly water) through the zeolite matrix comprises of three steps: (i) strong adsorption of the species into a cage from feed side, (ii) surface diffusion of the species from cage to cage and (iii) vaporization of the species to permeate side. Normally, any physical adsorption process includes both van der Waals dispersion-repulsion forces and electrostatic forces comprising of polarization, dipole and quadrupole interactions. However, since the zeolites have an ionic structure, the electrostatic forces become very large in adsorption of polar molecules like H₂O. This effect is manifested in the fact that heat of adsorption of water into zeolitic adsorbents is unusually high (25–30 kcal/mole). Researchers have extended the dusty-gas model approach to describe the surface-diffusion of molecules into a zeolite surface. The vacant sites are assumed to be the (n+1) pseudo-species in the system and S.M. Equation is used to correlate surface chemical potential gradient to flux of the various species, as shown in Eq. (1):

$$-\nabla\mu_i = RT \sum_{k=1}^n \theta_k \frac{(v_i - v_{n+1})}{D_{ik}^s} + RT \theta_{n+1} \frac{(v_i - v_{n+1})}{D_{i,n+1}^s}, \quad i = 1, 2, \dots, n \quad (1)$$

For two components denoted by 1 and 2, diffusing in a zeolite pore where the vacant sites are represented by v, individual component equations can be written as shown in Eqs. (2) And

(3) (velocity of the sites v_v is equal to 0). It is also conventional to define surface diffusivity D_{iv}^s as the ratio of $D_{i,n+1}^s$ and θ_{n+1}

$$-\frac{\nabla\mu_1}{RT} = \left[\frac{\theta_2(v_1 - v_2)}{D_{12}^s} + \frac{v_1}{D_{1v}^s} \right] \quad (2)$$

$$-\frac{\nabla\mu_2}{RT} = \left[\frac{\theta_1(v_2 - v_1)}{D_{21}^s} + \frac{v_2}{D_{2v}^s} \right] \quad (3)$$

Surface flux of each species through the zeolite pore is represented by Eqs. (4) And (5), where ρ_p is density of the zeolite, ε is porosity, q_{sat}^i is maximum possible sorption of component i into the zeolite, θ_i is site occupancy of species i and v_i is velocity of component i through the pores.

$$J_1^s = \rho_p \varepsilon q_{sat}^1 \theta_1 v_1 \quad (4)$$

$$J_2^s = \rho_p \varepsilon q_{sat}^2 \theta_2 v_2 \quad (5)$$

Assuming that there is no counter diffusion or coupling between the two species (D_{12}^s and $D_{21}^s \rightarrow \infty$), Eqs. (2) And (3) can be further simplified to Eqs. (6) and (7):

$$-\frac{\nabla\mu_1}{RT} = \frac{J_1^s}{\rho_p \varepsilon q_{sat}^1 \theta_1 D_{1v}^s} \quad (6)$$

$$-\frac{\nabla\mu_2}{RT} = \frac{J_2^s}{\rho_p \varepsilon q_{sat}^2 \theta_2 D_{2v}^s} \quad (7)$$

From basic thermodynamics, chemical potential gradients ($\nabla\mu_1$ and $\nabla\mu_2$) can be represented as gradients of the site occupancy of each species by the following equations:

$$-\frac{\theta_1 \nabla\mu_1}{RT} = \theta_1 \frac{\partial \ln a_1}{\partial \theta_1} \frac{d\theta_1}{dz} + \theta_1 \frac{\partial \ln a_1}{\partial \theta_2} \frac{d\theta_2}{dz} \quad (8)$$

$$-\frac{\theta_2 \nabla\mu_2}{RT} = \theta_2 \frac{\partial \ln a_2}{\partial \theta_2} \frac{d\theta_2}{dz} + \theta_2 \frac{\partial \ln a_2}{\partial \theta_1} \frac{d\theta_1}{dz} \quad (9)$$

Equating Eqs. (6) And (8) with Eqs. (7) and (9):

$$J_1^s = -\rho_p \varepsilon q_{sat}^1 D_{1v}^s \left[\theta_1 \frac{\partial \ln a_1}{\partial \theta_1} \frac{d\theta_1}{dz} + \theta_1 \frac{\partial \ln a_1}{\partial \theta_2} \frac{d\theta_2}{dz} \right] \quad (10)$$

$$J_2^s = -\rho_p \varepsilon q_{sat}^2 D_{2v}^s \left[\theta_2 \frac{\partial \ln a_2}{\partial \theta_2} \frac{d\theta_2}{dz} + \theta_2 \frac{\partial \ln a_2}{\partial \theta_1} \frac{d\theta_1}{dz} \right] \quad (11)$$

The above two equations describe flux of each component through the zeolite pore. Nature of the functions $\left(\frac{\partial \ln a_i}{\partial \theta_i}\right)$,

$\left(\frac{\partial \ln a_1}{\partial \theta_2}\right)$, $\left(\frac{\partial \ln a_2}{\partial \theta_1}\right)$ and $\left(\frac{\partial \ln a_2}{\partial \theta_2}\right)$ depends on nature of the sorption isotherm of each compound into the zeolite. Diffusivities D_{1v}^s and D_{2v}^s are also dependent on the site occupancies θ_1 and θ_2 . Thus, to be able to model flux of each component through the zeolite cages, knowledge of both diffusion and sorption characteristics is essential. For zeolites with narrow pores (as in the case of zeolite NaA), single file diffusion can be assumed to take place. In the case of single file diffusion, only one molecule can diffuse through the cross-section of the pore at any given time. The S.M. surface diffusivity (D_{1v}^s) depends linearly on the vacant sites (θ_v) as shown below:

$$D_{1v}^s = D_{1v}^s(0)\theta_v \quad (12)$$

A Langmuirian type of sorption isotherm (for pure water into zeolite sites) to predict activity (a_w) in the zeolite for a given site occupancy (θ_w) can be assumed:

$$a_w = \frac{A\theta_w}{1 - \theta_w} \quad (13)$$

For pure water-zeolite system, there is no second component and Eqs. 11-13 can be used to obtain the pure water flux equation as:

$$J_w^s = \rho \varepsilon q_{sat}^w D_{wv}^s(0) \frac{d\theta_w}{dz} \quad (14)$$

Integrating the above equation between the limits

$$z = 0, q_w = q_{w,f} \quad \text{and} \quad z = \delta, \theta_w = \theta_{w,p} :$$

$$J_w^s = \frac{\rho \varepsilon q_{sat}^w D_{wv}^s(0)}{\delta} (\theta_{w,f} - \theta_{w,p}) \quad (15)$$

Multiplying q_{sat}^w by the terms in the bracket, the final flux equation is:

$$J_w^s = \frac{\rho \varepsilon D_{wv}^s(0)}{\delta} (q_{w,f} - q_{w,p}) \quad (16)$$

Where $q_{w,f}^w$ and $q_{w,p}^w$ are the sorbet quantities of water into the zeolite at the feed and the permeate interfaces. The above equation is based on the premise that transport of various species through a dense zeolite membrane follows the solution-diffusion mechanism. It should be mentioned that zeolite membranes obey a sorption diffusion model like polymeric membranes; however, the ionic interactions are stronger in the case of zeolite membranes. The ionic interactions affect both the sorption and the diffusion of water into the membrane. For the zeolite membranes, a solution-diffusion mechanism can be envisioned wherein the water molecules first adsorb preferentially at the cage mouth and then diffuse across the active layer. For solvent molecules, however, the partial molecular sieving effects and permeation through non-zeolitic

pores may also need to be considered. Therefore, a permeability parameter K_w can also be defined for water permeation through zeolite membranes in a similar manner as for polymeric membranes. The parameter is a lumped parameter comprising of the water diffusivity through the membrane, its sorption onto the membrane material and the membrane thickness. The above equation assumes that the permeability parameter remains constant under various feed concentrations and temperatures. However, this is not always true, especially in the case of polymeric membranes. For example, hydrophilic polymeric membranes tend to swell substantially in the presence of high water concentrations causing substantial changes in the permeability parameter of the polymer. The above model is a comprehensive modeling approach and gives helpful insights into the actual transport process within nanopores of the zeolite [22-25].

3.2 Water sorption experiments

The sorption experiments were performed using zeolite powder (200-mesh size). The zeolite powder in the presence of pure water forms a paste and it is very difficult to distinguish between the 'sorbet water' and the 'inter-particle water'. Thus, any sorption data based on gravimetric studies is not expected to be accurate. An indirect and more accurate method was employed to determine the pure water sorption of the zeolite powder. The zeolite powder was weighted and the powder was well mixed with a measured volume of the dilute UDMH mixture (1, 5, 10, 15 and 20 wt %). Equilibrium was established after 18–24 h. After the equilibrium, the mixtures were pressure filtered using a syringe. The water content was accurately measured. It was assumed that at such low UDMH concentrations, sorption of UDMH into the zeolite powder is negligible. The results were presented in Table 5.

3.3 Water flux calculation using S.M. Correlation

After water sorption experiments, Eq. (16) was employed to calculate diffusivity values of water through the zeolite matrix at 25°C using water flux and sorption values at the same temperature. The diffusivity of pure water through the zeolite at 25°C was computed (assuming $q_{w,p} = 0$, $\rho_s = 1990 \text{ kg/m}^3$, $\varepsilon = 0.49$ and $\delta = 30 \mu\text{m}$ to be $3.11 \times 10^{-8} \text{ cm}^2/\text{s}$ (using experimental value of $J_w = 0.22 \text{ kg/m}^2 \cdot \text{h}$ and $q_{w,p} = 0.6 \text{ kg/kg}$ zeolite at 25°C). Sorption studies were also carried out using the zeolite NaA membrane. The zeolite membrane was crushed into fine pieces and the sorption experiments were performed in a similar manner as the powder. The sorption of the zeolite membrane was measured to be 0.29 kg/kg zeolite again indicating that the membrane is highly hydrophilic. This value is lower than the values of water sorption for the zeolite powder because of the backing material. The results of water flux calculations were also presented in Table 5.

Comparison of experimental water fluxes and calculated water fluxes by S.M. Correlation were demonstrated in Table 5 and Figure 16. Variation of the experimental flux through the

zeolite membranes and the calculated flux with water concentration in the feed mixtures was shown. As seen in Table 5 and Figure 16, reduction of water content in the mixture causes the water flux to decrease. As seen, the experimental and calculated data are consistent.

4. Conclusion

Zeolite membranes have great potential for applications in UDMH dehydration. ZSM-5, NaY, NaX, Mordenite and NaA Zeolite membranes were synthesized on the porous mullite tubes by hydrothermal method. NaA Zeolite membrane showed the best separation factor for dehydration of these mixtures. The presented model in this research is a comprehensive modeling approach and gives helpful insights into the actual transport process within nanopores. The water flux through the membrane was found to be almost independent on the UDMH concentration (at high water concentrations 80–100 wt %) implying that the water transport through the membrane is uncoupled.

References

- [1] Buekenhoudt, A., C. Dotremont, V. Van Hoof, Performance of Mitsui NaA type zeolite membranes for the dehydration of organic solvents in comparison with commercial Polymeric pervaporation membranes, Separation and Purification Technology 48 (2006) 304–309.
- [2] Churl, H, Y. Ka, G. Jeong, K. Si, M. Young, Synthesis, ethanol dehydration and thermal stability of NaA layer zeolite/a;umina composite membrane with narrow non zeolitic pores and thin intermediate, Journal of Membrane Science, 364 (2010) 138–148.
- [3] Zhen Huang, Yan Shi, Rui Wen, Yu-Hua Guo, Jun-Feng Su, T. Matsuura, Multilayer poly(vinyl alcohol)–zeolite 4A composite membranes for ethanol dehydration by means of pervaporation, Separation and Purification Technology 51 (2006) 126–136.
- [4] Khan, A., G. Susheela, G. J. Reddy, S. Sridhar, Cross linked chitosan membranes: characterization and study of dimethylhydrazine dehydration by pervaporation, Polymer International, 50, 1156–1165 (2001).
- [5] Khan, A., A. K. Rao, K. R. Krovvidi, R. Ravindra, and D.S.C. studies of states of water, hydrazine and hydrazine hydrate in ethyl cellulose membrane, Polymer 40 (1999) 1159–1165.
- [6] Siddhartha M, K. Praveen, S. Bohra, S. Sridhar, Pervaporation performance of PPO membranes in dehydration of highly hazardous mmh and udmh liquid propellants, Journal of Hazardous Materials 288 (2015) 69–79.
- [7] Sonia Aguado, Jorge Gascn, Jacobus C. Jansen, Freek Kapteijn, Continuous synthesis of NaA zeolite membranes, Micro porous and Mesoporous Materials 120 (2009) 170–176.
- [8] A. Malekpour, M.R. Millani, M. Kheirkhah, Synthesis and characterization of a NaA zeolite membrane and its applications for desalination of radioactive solutions, Desalination 225 (2008) 199–208.
- [9] K. Speronello., 1986- Porous mullite, U.S. Patent NO 4628042.
- [10] K. Speronello., 1986- Porous mullite, U.S. Patent No. 4601997.
- [11] Weiguo Sun, Xianwu Wang, Jianhua Yang, Jinming Lu, Huilin Han, Yan Zhang, Jinqu Wang, Pervaporation separation of acetic acid–water mixtures through Sn-substituted ZSM-5 zeolite membranes, Journal of Membrane Science 335 (2009) 83–88.

- [12] Hannes R., Hartwig V., I. Voigt, A. Diefenbacher, G. Schuch, F. Steinbach, J. Caro, High-flux ZSM-5 membranes with an additional non-zeolite pore system by alcohol addition to the synthesis batch and their evaluation in the 1-butene/i-butene separation, Separation and Purification Technology 72 (2010) 388–394
- [13] Pinghai S., A. Kumar, Separation of 1-butanol/2, 3-butanediol using ZSM-5 zeolite-filled polydimethylsiloxane membranes, Journal of Membrane Science 339 (2009) 143–150
- [14] Shifeng, N., X. Liu, W. Liu, B. Zhang, Ethanol recovery from its dilute aqueous solution using Fe-ZSM-5 membranes: Effect of defect size and surface hydrophobicity, Microporous and Mesoporous Materials 215 (2015) 46-50.
- [15] Avila, A, Z. Yu, S. Fazli, J. Sawada, S. Kuznicki, Hydrogen-selective natural mordenite in a membrane reactor for ethane dehydrogenation, Microporous and Mesoporous Materials, 190(2014) 301-308.
- [16] Sorenson, S, E. Payzant, W. Gibbons, B. Soydas, H. Kita, R. Noble, J. Falconer, Influence of zeolite crystal expansion/contraction on NaA zeolite membrane Separations, Journal of Membrane Science 366 (2011) 413–420.
- [17] Caro, J, D. Albrecht, M. Noack, Why is it so extremely difficult to prepare shape-selective Al-rich zeolite membranes like LTA and FAU for gas separation? Separation and Purification Technology 66 (2009) 143–147.
- [18] Algieri, C, P. Bernardo, G. Barbieri, E. Drioli, novel seeding procedure for preparing tubular NaY zeolite membranes, Microporous and Mesoporous Materials 119 (2009) 129–136.
- [19] Mirza, A, B. Patel, K. Alhooshani, O. Muraza, E.Wang, T. Laoui, In-situ aging microwave heating synthesis of LTA zeolite layer on mesoporous TiO₂ coated porous alumina support, Journal of Crystal Growth, 432 (2015) 123-128.
- [20] Fedosov, D, A. Smirnov, V. Shkirskiy, T. Voskoboinikov, I. Ivanova, Methanol dehydration in NaA zeolite membrane reactor, Journal of Membrane Science, 486 (2015)189-194
- [21] Pera-Titus, M., R. Mallad, Preparation of inner-side tubular zeolite NaA membranes in a semi-continuous synthesis system, Journal of Membrane Science 278 (2006) 401–409.
- [22] Hogendoorn, J, van der Veen, A, van der Stegen., Application of the Maxwell–Stefan theory to the membrane electrolysis process Model development and simulations, Computers and Chemical Engineering 25 (2001) 1251–1265.
- [23] Krishna, R, Paschek, D, Verification of the Maxwell–Stefan theory for diffusion of three-component mixtures in zeolites, Chemical Engineering Journal 87 (2002) 1–9.
- [24] Llorens, J., M. Pera-Titus, Description of the pervaporation dehydration performance Of A-type zeolite membranes: A modeling approach based on the Maxwell–Stefan theory, Catalysis Today 118 (2006) 73–84.
- [25] S. Amnuaypanich, J.Patthana, P.Phinyocheep, Mixed matrix membranes prepared from natural rubber/poly(vinyl alcohol) semi- interpenetrating polymer network (NR/PVA semi-IPN) incorporating with zeolite 4A for the pervaporation dehydration of water–ethanol mixtures, Chemical Engineering Science 64 (2009) 4908 – 4918.

Table 1: Energy requirements for ethanol dehydration

Purification (Wt. %)	Energy required (kJ/kg EtOH)	Process
8.0–99.5	10376	Distillation
95.0–99.5	3305	Azeotropic distillation
95.0–99.5	423	Pervaporation

Table 2: Analysis of kaolin clay

Component	Percent (%)	Phases	Percent (%)
SiO ₂	51.9	Kaolinite	79
TiO ₂	0.1	Illite	8
Al ₂ O ₃	34.1	Quartz	10
Fe ₂ O ₃	1.4	Feldspar	3
K ₂ O	0.8	Total	100
Na ₂ O	0.1		
L.O.I	11.6		
Total	100		



Figure 1: Mullite support

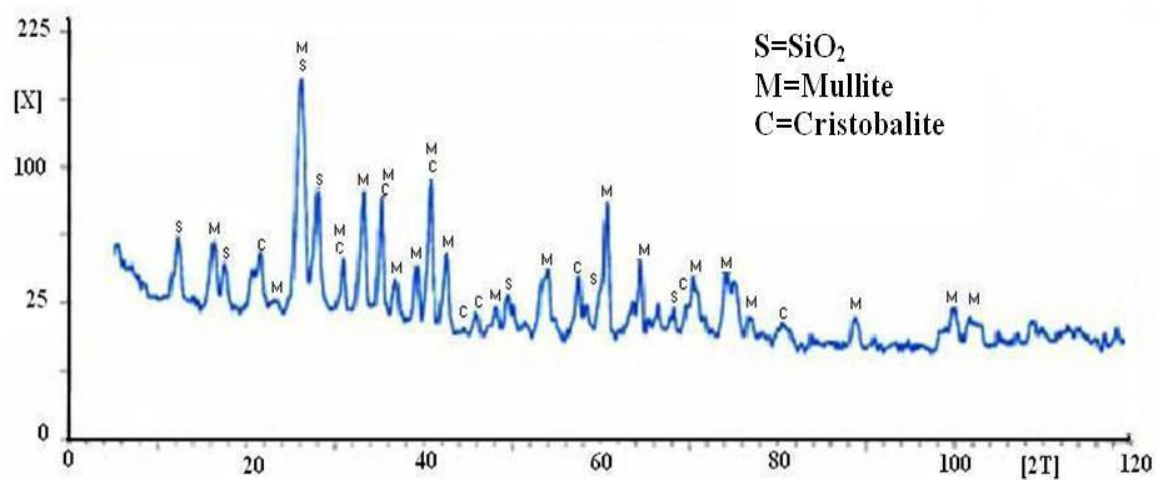


Figure 2: XRD patterns of the support

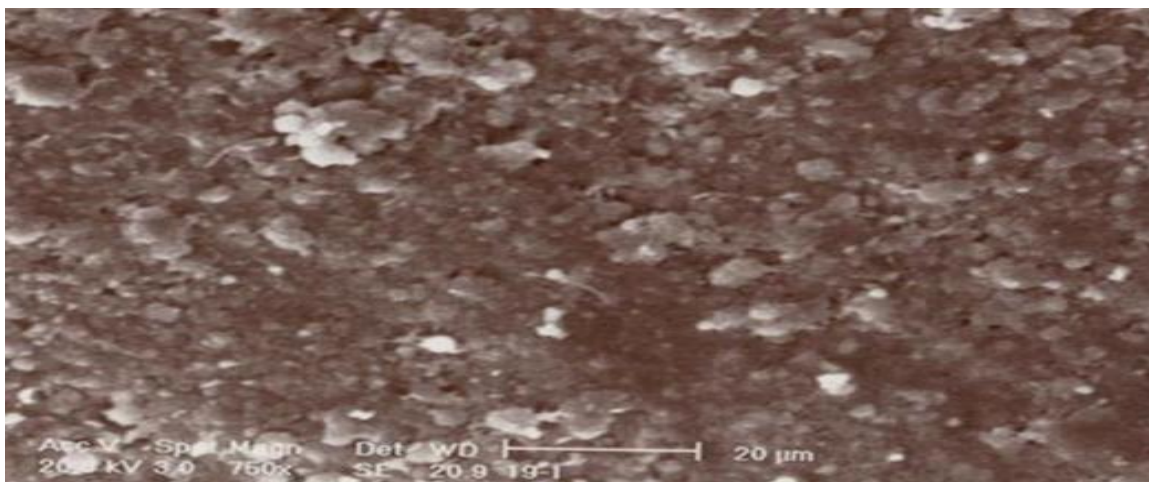


Figure 3: SEM micrograph of a) the support

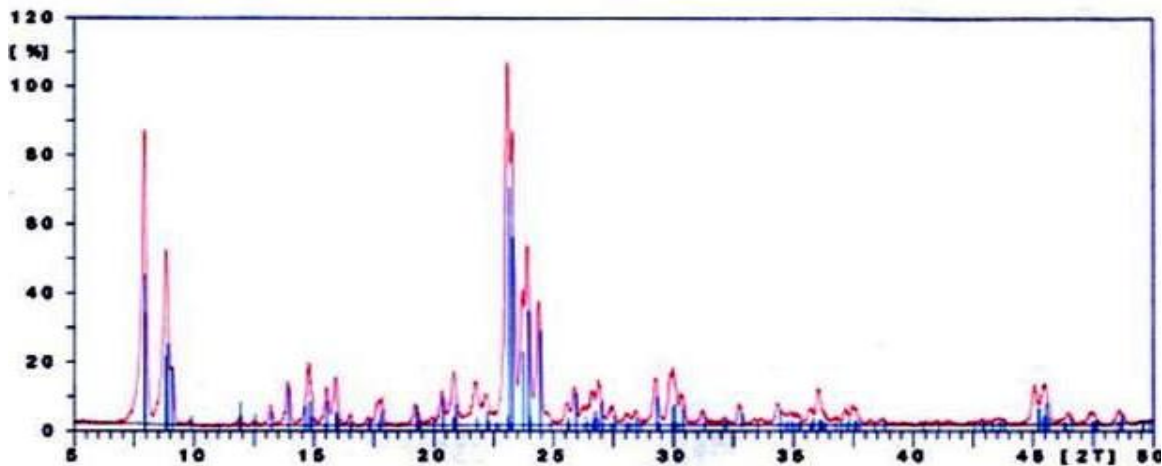


Figure 4: XRD patterns of the ZSM-5 zeolite membrane

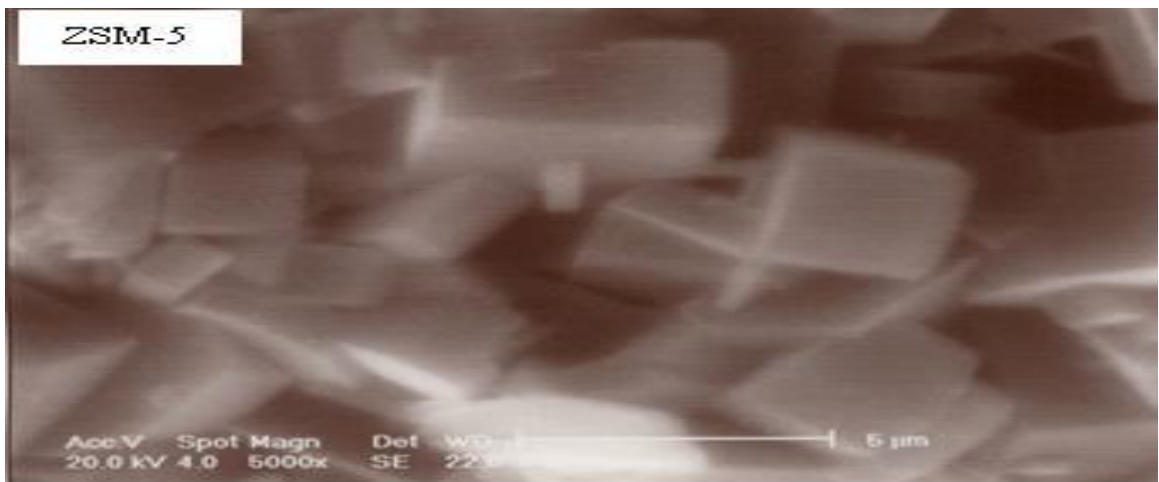


Figure 5: SEM micrograph of the ZSM-5 zeolite membrane

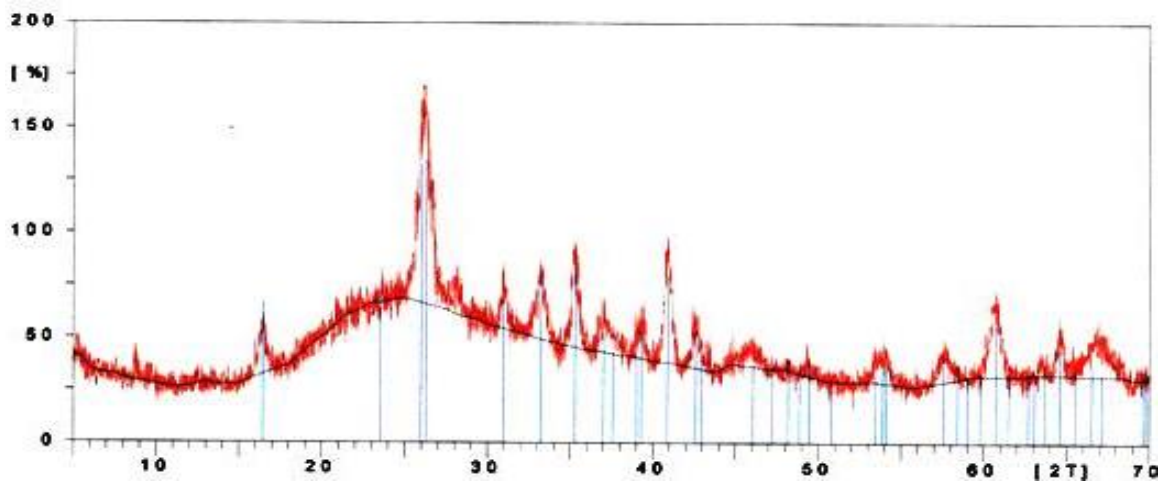


Figure 6: XRD patterns of the Mordenite zeolite membrane

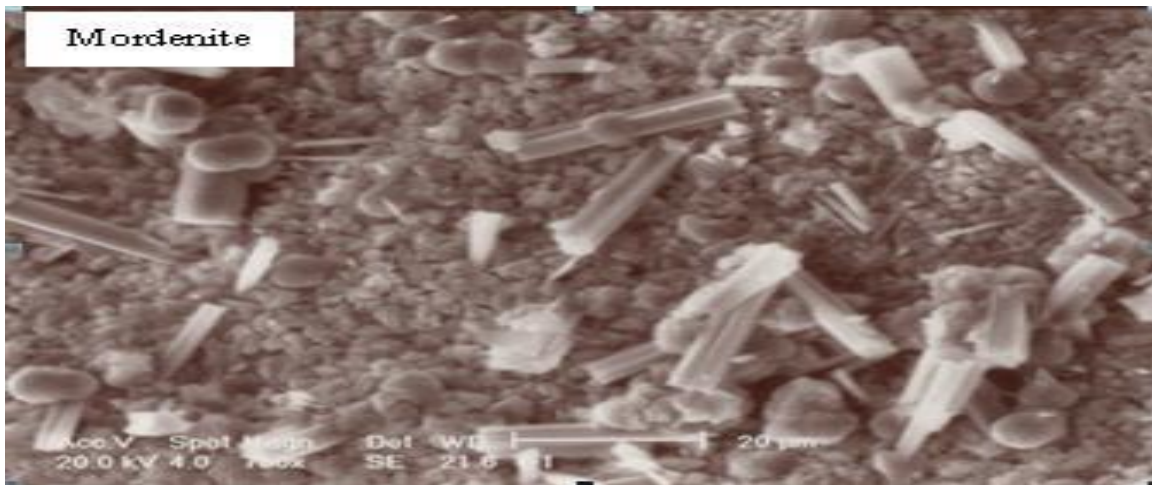


Figure 7: SEM micrograph of the Mordenite zeolite membrane

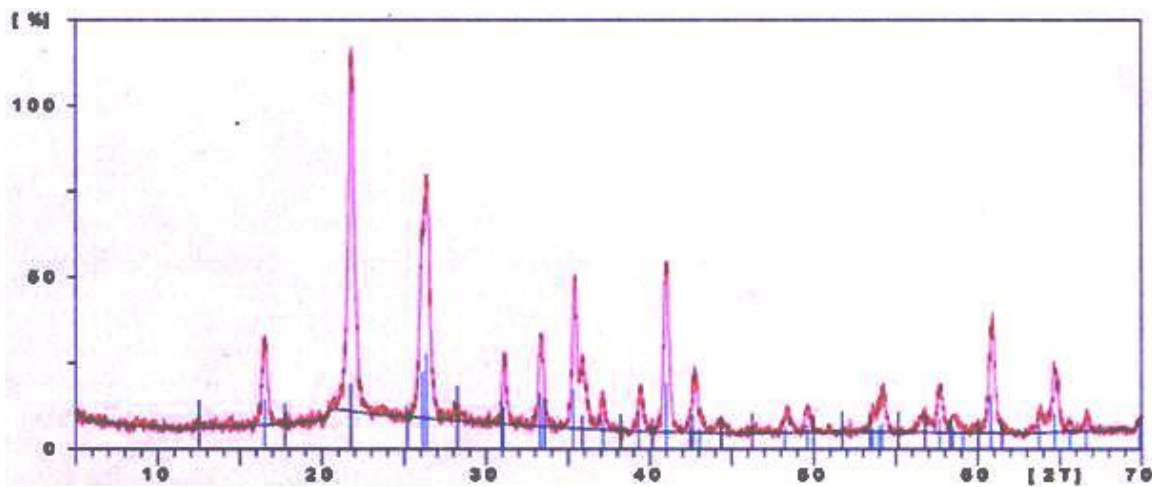


Figure 8: XRD patterns of the NaX zeolite membrane

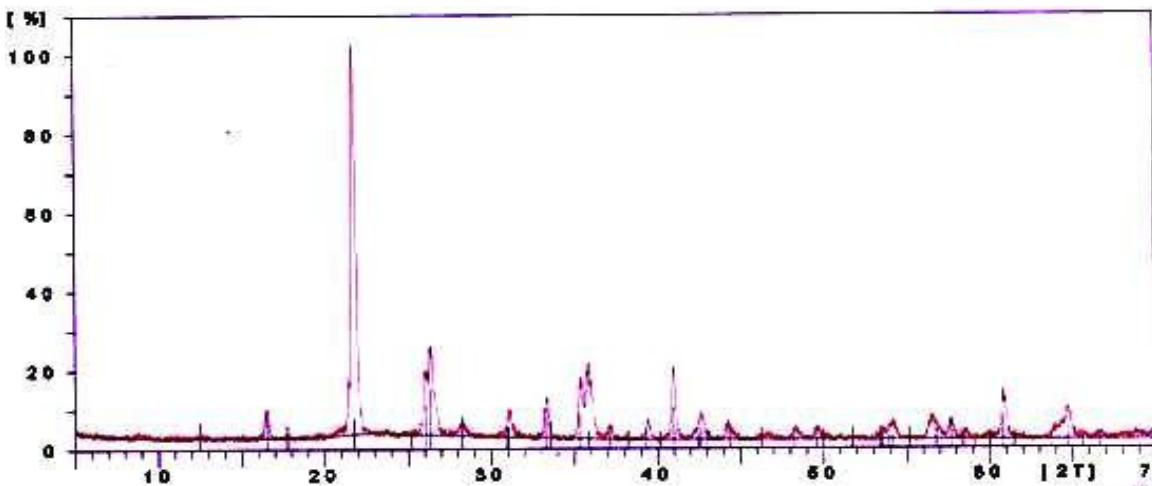


Figure 9: XRD patterns of the NaY zeolite membrane

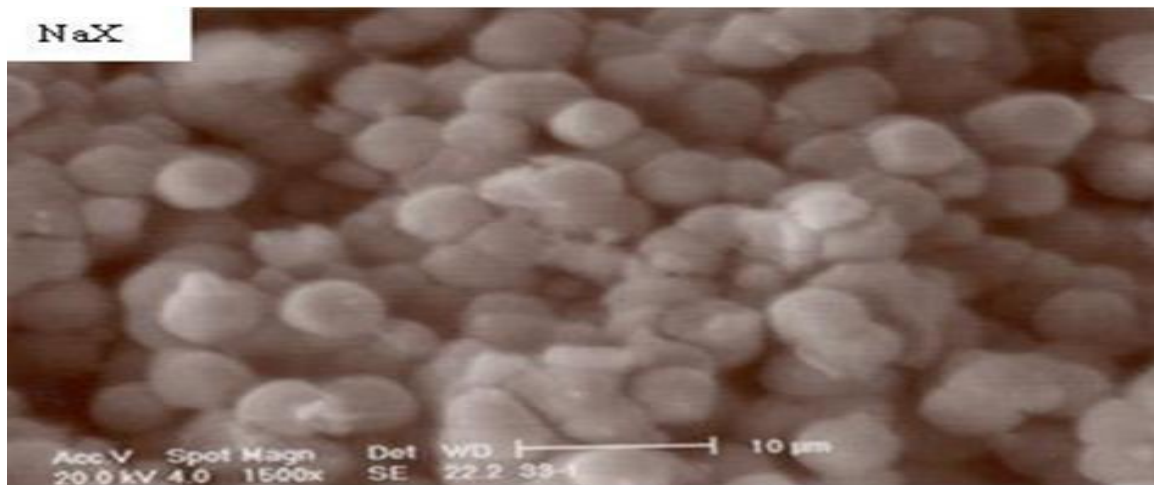


Figure 10: SEM micrograph of the NaX zeolite membrane

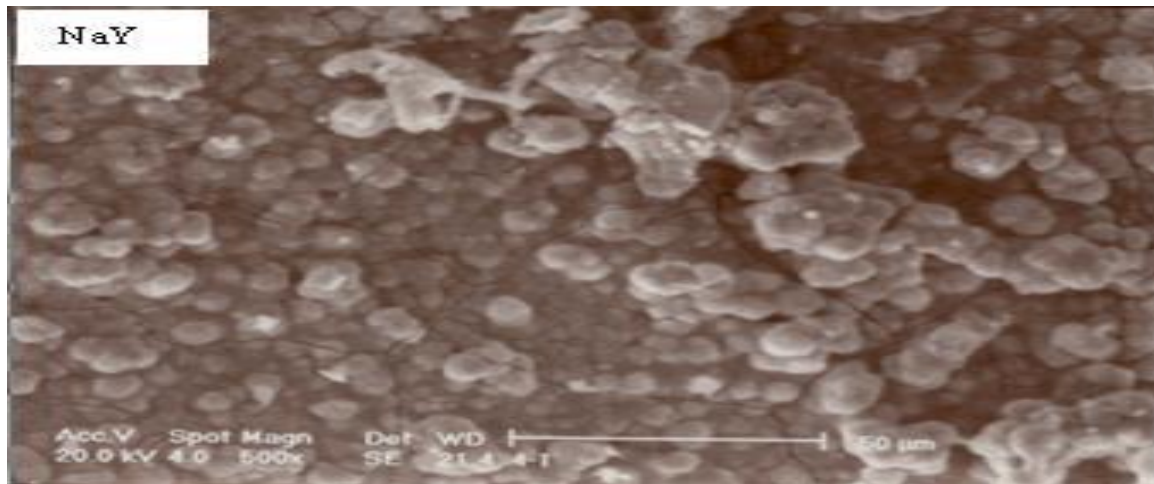


Figure 11: SEM micrograph of the NaY zeolite membrane

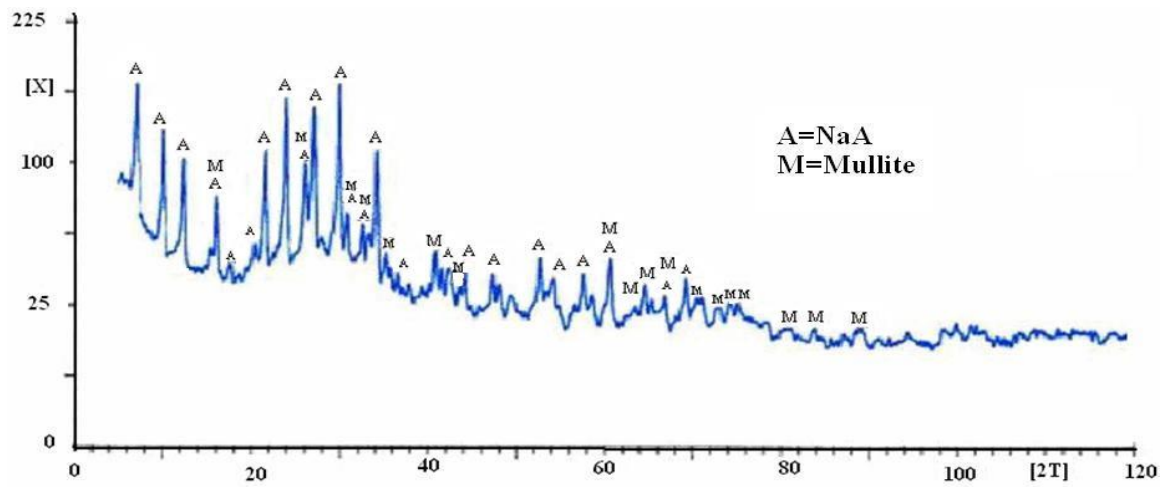


Figure 12: XRD patterns of support and membrane

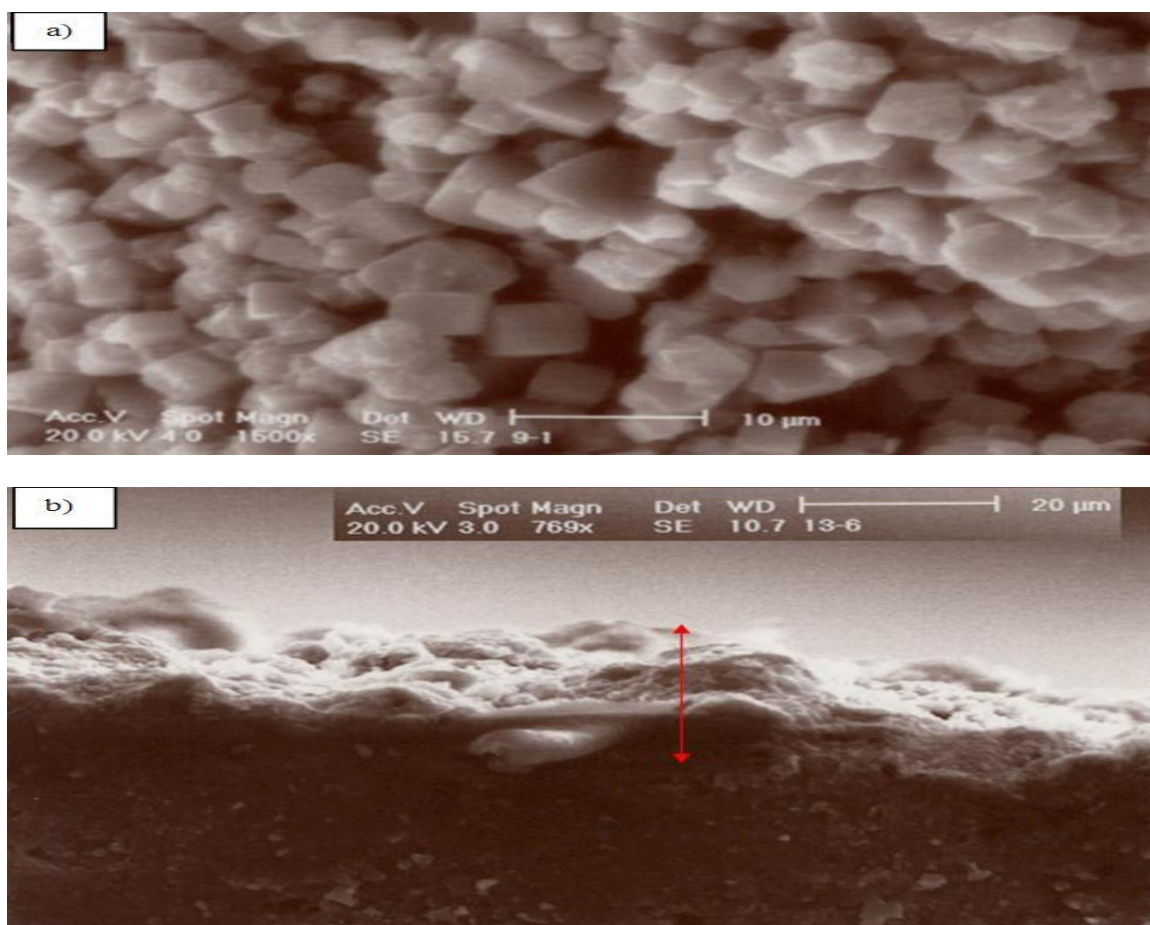


Figure 13: SEM micrograph of a) the membrane (surface) b) the membrane (cross section)

Table 3: Gel formulations of zeolite membranes

Sample	Zeolite membrane	Gel formulation
1	NaX	5.0Na ₂ O: 1.0Al ₂ O ₃ : 4.0SiO ₂ : 150H ₂ O
2	ZSM-5	0.292Na ₂ O: 1.0Al ₂ O ₃ : 100SiO ₂ : 2.0TPABr 40H ₂ O
3	NaY	4.0Na ₂ O: 1.0Al ₂ O ₃ : 10SiO ₂ : 250H ₂ O
4	Mordenite	9.75Na ₂ O: 1.0Al ₂ O ₃ : 9.0SiO ₂ : 780H ₂ O
5	NaA	1.926 SiO ₂ : Al ₂ O ₃ : 3.165 Na ₂ O: 128 H ₂ O

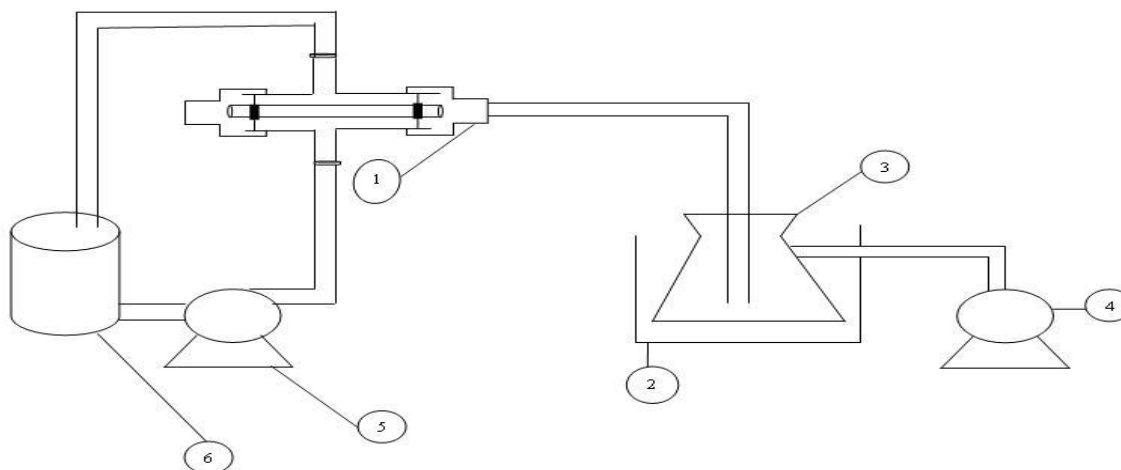


Figure 14: PV setup; 1- feed container and PV cell 2- liquid nitrogen trap 3- permeate container 4- three-stage vacuum pump 5- centrifuge pump 6- feed tank

Table 4: Flux and separation factors of zeolite membranes

S.No	Zeolite membrane	Feed concentration (%)	Flux(kg/m ² .h)	Separation Factor
1	NaX	5	1.34	40
2	ZSM-5	5	0.67	55
3	NaY	5	0.27	72
4	Mordenite	5	2.14	264
5	NaA	5	0.31	10000
6	NaX	2	0.62	10000

Truncated Octahedrons (β -cages)

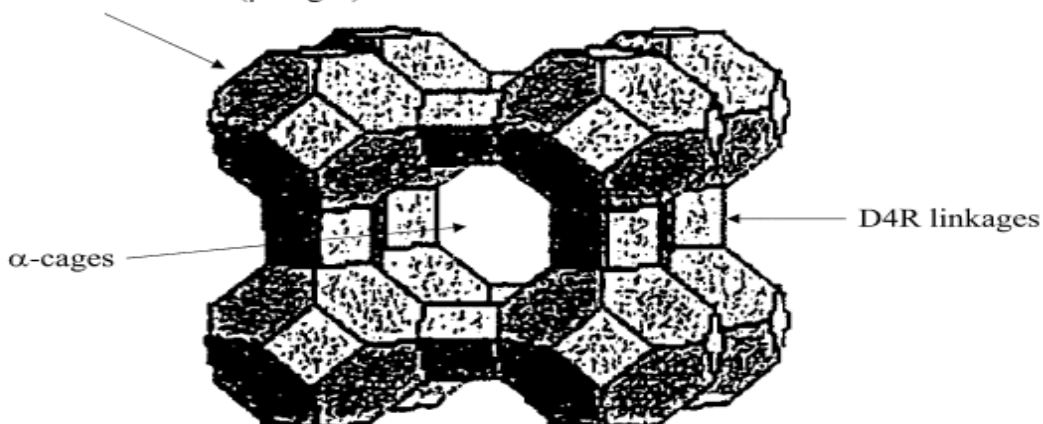


Figure 15: Repeating unit of zeolite NaA

Table 5: Experimental and calculated data for NaA zeolite membrane

S.No	UDMH Con. (%)	$q_{w,f}$: kg/kg zeolite	J(Cal.) (kg/m ² .h)	J (Exp.) (kg/m ² .h)
1	1	0.589	0.334	0.329
2	5	0.560	0.317	0.304
3	10	0.511	0.289	0.269
4	15	0.473	0.268	0.248
5	20	0.432	0.245	0.215

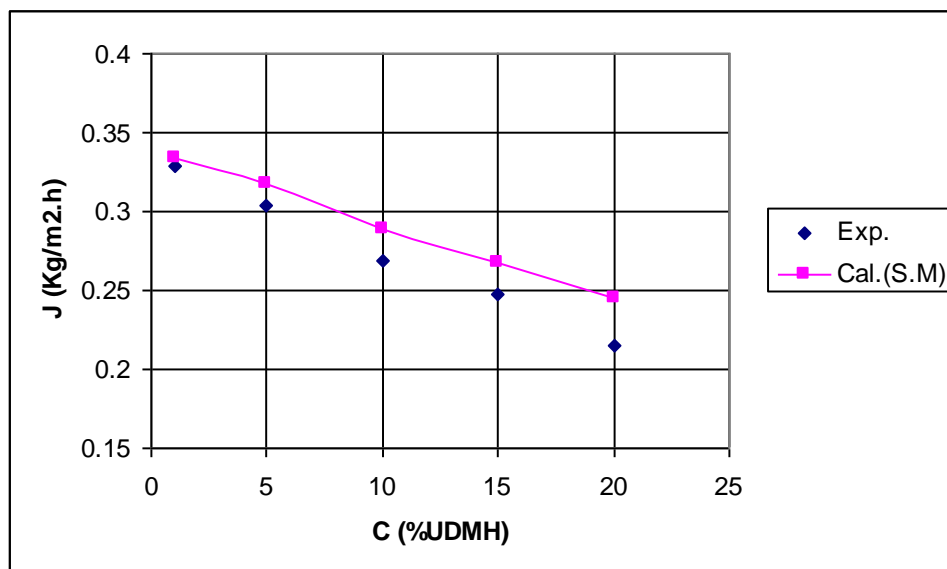


Figure 16: Water flux as a function of UDMH concentration